AIMS Mathematics

http://www.aimspress.com/journal/Math

AIMS Mathematics, 6(8): 8742–8771.
DOI: 10.3934/math.2021508
Received: 11 March 2021
Accepted: 20 May 2021
Published: 09 June 2021

Research article

A new integral operational matrix with applications to multi-order fractional differential equations

Imran Talib[1,*], Md. Nur Alam[2], Dumitru Baleanu[3,*], Danish Zaidi[4] and Ammarah Marriyam[1]

[1] Nonlinear Analysis Group (NAG), Mathematics Department, Virtual University of Pakistan, Pakistan

[2] Department of mathematics, Pabna University of science and technology, Pabna-6600, Bangladesh

[3] Cankaya University, Department of Mathematics and Computer Sciences, Ankara

[4] Department of Mathematics, University of Management and Technology, Lahore, Pakistan

* **Correspondence:** Email: dumitru.baleanu@gmail.com, imrantaalib@gmail.com; Tel: +923227268580.

Abstract: In this article, we propose a numerical method that is completely based on the operational matrices of fractional integral and derivative operators of fractional Legendre function vectors (FLFVs). The proposed method is independent of the choice of the suitable collocation points and expansion of the residual function as a series of orthogonal polynomials as required for Spectral collocation and Spectral tau methods. Consequently, the high efficient numerical results are obtained as compared to the other methods in the literature. The other novel aspect of our article is the development of the new integral and derivative operational matrices in Riemann-Liouville and Caputo senses respectively. The proposed method is computer-oriented and has the ability to reduce the fractional differential equations (FDEs) into a system of Sylvester types matrix equations that can be solved using *MATLAB* builtin function *lyap*(.). As an application of the proposed method, we solve multi-order FDEs with initial conditions. The numerical results obtained otherwise in the literature are also improved in our work.

Keywords: Riemann-Liouville integral operational matrix; Caputo derivative operational matrix; fractional Legendre function vectors; multi-order fractional differential equations; fully operational matrices approach
Mathematics Subject Classification: 65M99, 26A33, 35R11, 45K05

1. Introduction

Fractional calculus (FC) is a study of derivatives and integration of arbitrary order. At the initial phases of its development, it was considered an abstract mathematical idea with nearly no applications. But, now the situation is entirely different with FC and is considered to be the most useful and important topic among the scientific community. The various important phenomena of science and engineering have been well described with the use of fractional derivatives, including, partial bed-load transport, diffusion model, dynamics of earthquakes, viscoelastic systems, biological systems, chaos, and wave propagation, (see [1–3, 7–10, 41, 42]) and references therein. The nonlocal property of the fractional operators makes them more efficient for modeling the various problems of physics, fluid dynamics and their related disciplines, (see [17, 18, 43, 44]).

Most of the classical (integer order) and FDEs are not possible to solve analytically, therefore, some reliable numerical methods and semi-analytical methods have been developed to solve them. Some of them are presented as follows: In [34], the authors extended the study of [45] to solve numerically the Caputo type tempered fractional integro-differential equations. In [36], the authors solved the various kind of Riemann problems by developing a mixed-method, namely, the characteristic Adomian decomposition method (CADM) which is the improved form of ADM. In [38], the authors constructed the power series solution of the time-fractional Majda-Biello system by applying the Lie group analysis. For more information on Lie group analysis and its applications, (see [35]). In [39], the authors investigated the behaviour of cavitation models together with thermodynamic effects by developing a compressible, two-phase, one-fluid Navier-Stokes solver. In [40], the authors presented the analytical and computational study of the drift-flux two-phase flow model. The analytical solution of the model is based on the analytical solution of the Riemann problem which consists of two different nonlinear algebraic equations in velocity equilibrium and pressure nonequilibrium between the two-phase systems. The numerical solution is obtained by using the finite volume methods. In [37], the authors implemented a void ratio transport-equation model in a one-fluid two-phase compressible software by proposing a various numerical techniques which are based on a finite volume approach, including, HLLC, Rusanov, VF Roe, Jameson-Schmidt-Turkel and AUSM. For more detail on transport-equation and its applications, (see [33]). In [43], the authors proposed the fully discretized finite element approximations to solve the time-fractional diffusion equations of variable-order.

Orthogonal polynomials coupled with operational matrices of fractional derivatives operators defined with singular or nonsingular kernels have played a significant role in the development of the spectral methods. The most commonly used methods are Spectral tau methods, and Spectral collocation methods. These methods have been successfully used to find the approximate solution of a large class of multi-order ordinary and partial FDEs. Some of them are presented as follows: In [13], the authors solved the multi-order (MOFDEs) by combining the technique of operational matrices with Spectral tau and Spectral collocation methods. In [14], the authors solved the MOFDEs by using the Chebyshev operational matrix (COM) together with Spectral tau and Spectral collocation methods. In [15], the authors solved the MOFDEs by reducing them into a system of FDEs, then combining the COM with Spectral tau and Spectral collocation methods. In [19], the authors derived the derivative operational matrix in Caputo sense of FLFVs which then applied with Spectral tau method to solve MOFDEs. In [20], the authors derived the integral COM in Riemann-Liouville sense

which then applied with Spectral tau method to solve numerically the MOFDEs. In [22], the author derived the Jacobi integral operational matrix in Riemann-Liouville sense which then applied with Spectral tau method to solve MOFDEs. However, these methods have certain numerical difficulties in applying: in spectral tau methods, the residual function must be expanded as a series of orthogonal polynomials and then the initial or boundary conditions are applied as constraints; whereas in spectral collocation methods, the requirement of the choice of the suitable collocation points are necessary and FDEs must be satisfied exactly at these points.

In this article, we propose a numerical method which is completely based on the fractional derivative and integral operational matrices of FLFVs. The proposed method is independent of the choice of the suitable collocation points and expansion of the residual function as a series of orthogonal polynomials. Consequently, the proposed method produces high efficient numerical results as compared to the Spectral tau method [13], Bessel collocation method [6], Taylor matrix method [5], function approximation theory [21], and stochastic technique [4]. The other novel aspect of our article is the development of new integral and derivative operational matrices in Riemann-Liouville and Caputo senses respectively. As an applications of the proposed method, we solve various MOFDEs corresponding to initial conditions. Our approach has ability to reduce the MOFDEs into a system of Sylvester types matrix equations which can be solved using *MATLAB* built in function *lyap*(.). The rest of the article is organized as follows:

In Section 2, some preliminaries definitions of FC are recalled. In Section 3, the analytical expressions and some useful properties of CSLPs are reviewed. Moreover, in the same section some important properties of FLFVs and its analytical expression are recalled. In Section 4, the new generalized integral operational matrix and derivative operational matrix of FLFVs in the senses of Riemann-Liouville and Caputo are derived. In Section 5, based on the results of Section 4, a numerical method is proposed which is an excellent tool to solve numerically the MOFDEs corresponding to initial conditions. In Section 6, the validity and the efficiency of the proposed numerical method is tested by solving various examples and comparing the results with other methods in the literature. Some concluding remarks and future directions are given in Section 7.

2. Preliminary remarks on FC

Some important definitions and results are recalled in this section which are indispensable to construct the proposed numerical algorithm.

Definition 1. The (left-hand side) Riemann-Liouville integral of order $\Omega > 0$ is given as (see [12]):

$$ {}_{RL}J^{\Omega}u(x) = \frac{1}{\Gamma(\Omega)} \int_0^x (x-t)^{\Omega-1} u(t)dt, \quad x > 0. \tag{2.1} $$

Definition 2. The (left-hand side) Caputo derivative of order $\Omega > 0$ is given as (see [12]):

$$ {}_{C}\mathcal{D}^{\Omega}u(x) = \begin{cases} \frac{d^n u(x)}{dx^n}, & \Omega = n \in \mathbb{N}, \\ {}_{RL}J^{n-\Omega}u^{(n)}(x), & n-1 < \Omega < n\ ,\ n \in \mathbb{N}, \end{cases} \tag{2.2} $$

where n is an integer, $x > 0$, and $u(x) \in C^n[0, 1]$.

For the Caputo derivative, we have the following observations:

$$ {}_C\mathcal{D}^{\Omega}K = 0, \qquad K \text{ is a constant.} \tag{2.3} $$

$$ {}_C\mathcal{D}^{\Omega}x^{\mu} = \begin{cases} 0, & \text{for } \mu \in \mathbb{R}_+, \text{ and } \mu < \lceil\Omega\rceil, \\ \frac{\Gamma(\mu+1)}{\Gamma(\mu+1-\Omega)}x^{\mu-\Omega}, & \text{for } \mu \in \mathbb{R}_+, \text{ and } \mu \geq \lceil\Omega\rceil. \end{cases} \tag{2.4} $$

3. FLFVs and its properties

Many approximate techniques are available in the literature to solve numerically the FDEs but the most frequent used approach is the approximation of the solutions via series expansion of the type, $\sum_{k=0}^{M} d_k t^{k\Omega}$. Thus the choice of the appropriate orthogonal function of the type $\Psi(t) = \sum_{k=0}^{M} d_k t^{k\Omega}$ is very important to get the good approximate results.

In recent, the authors in [23] worked on the development of the fractional representation of the classical Legendre polynomials using the well-known Rodrigues formula. However, it is difficult to solve FDEs with this proposed fractional extension due to complexity involved in these functions, so in order to obtain the solution of FDEs, in a much simpler and efficient manner, Kazem and coauthors generated the orthogonal FLFVs based on the orthogonal CSLPs to find the approximate solutions of linear and nonlinear FDEs (see [19]). In this section, the definition and some useful properties of orthogonal CSLPs and its fractional extension are reviewed.

3.1. Classical Shifted Legendre Polynomials (CSLPs)

The following recurrence formulae is used to evaluate the orthogonal Legendre polynomials (LPs) on the interval of orthogonality $[-1, 1]$ (see [11]):

$$ R_{j+1}(x) = \frac{2j+1}{j+1}xR_j(x) - \frac{j}{j+1}R_{j-1}(x), \quad j = 1, 2, \cdots, \tag{3.1} $$

where

$$ R_0(x) = 1, \quad R_1(x) = x. $$

Now by setting, $x = 2t - 1$ in (3.1), the CSLPs on the interval of orthogonality $[0, 1]$ can be expressed as following, (see [11])

$$ R_j(t) = \frac{(2j+1)(2t-1)}{j+1}R_j(t) - \frac{j}{j+1}R_{j-1}(t), \quad j = 1, 2, \cdots, \tag{3.2} $$

where

$$ R_0(t) = 1, \quad R_1(t) = 2t - 1. $$

The analytical expression of (3.2) is as following

$$ R_j(t) = \sum_{r=0}^{j} a_{r,j}t^r, $$

where

$$a_{r,j} = (-1)^{r+j} \frac{\Gamma(1+r+j)}{\Gamma(1-r+j)(\Gamma(1+r))^2}. \tag{3.3}$$

The orthogonality conditions of CSLPs can be expressed as

$$\int_0^1 R_j(t)R_i(t) = \begin{cases} \frac{1}{2j+1}, & \text{for } j = i, \\ 0, & \text{for } j \neq i. \end{cases} \tag{3.4}$$

3.2. Analytical expression and properties of FLFVs

The orthogonal FLFVs is defined in the following relation by changing the variable, t with z^{Ω}, $\Omega \in \mathbb{R}^+$ in orthogonal CSLPs defined in (3.2). For our convenience, we use the notation $FR_j^{\Omega}(z)$ to represent the FLFVs $(R_j(z^{\Omega}))$.

$$FR_j^{\Omega}(z) = \frac{(2j+1)(2z^{\Omega}-1)}{j+1} FR_j^{\Omega}(z) - \frac{j}{j+1} FR_{j-1}^{\Omega}(z), \quad j = 1, 2, \cdots, \tag{3.5}$$

where

$$FR_0^{\Omega}(z) = 1, \quad FR_1^{\Omega}(z) = 2z^{\Omega} - 1.$$

The analytical representation of (3.5) is as following

$$FR_j^{\Omega}(z) = \sum_{q=0}^{j} a'_{q,j} z^{q\Omega},$$

where

$$a'_{q,j} = (-1)^{q+j} \frac{\Gamma(1+q+j)}{\Gamma(1-q+j)(\Gamma(1+q))^2}. \tag{3.6}$$

The orthogonality conditions of FLFVs can be expressed as

$$\int_0^1 FR_j^{\Omega}(z) FR_i^{\Omega}(z) w(z) dz = \begin{cases} \frac{1}{\Omega(2j+1)}, & \text{for } j = i, \\ 0, & \text{for } j \neq i, \end{cases} \tag{3.7}$$

where $w(z) = z^{\Omega-1}$ is a weight function.

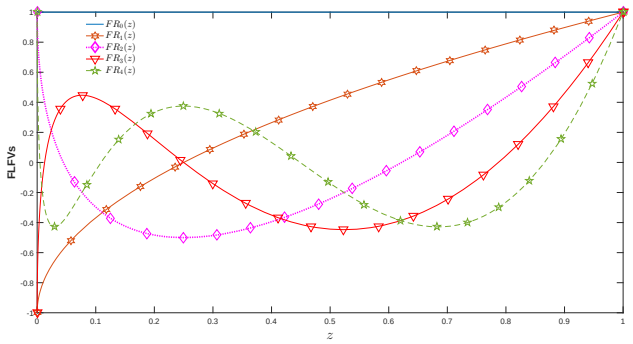

Figure 1. FLFVs are plotted for $\Omega = 1/2$ and for various choices of n.

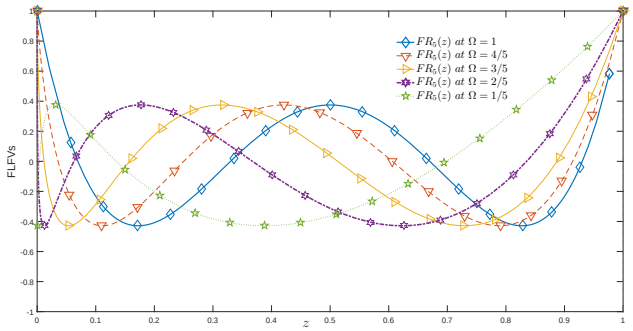

Figure 2. FLFVs are plotted taking $n = 4$ and for various choices of Ω.

3.3. Functions approximation using FLFVs

If $u(z) \in L^2[0, 1]$, then it can be demonstrated as a series expansion of orthogonal FLFVs, as

$$u(z) = \sum_{j=0}^{\infty} e_j FR_j^{\Omega}(z). \tag{3.8}$$

Using (3.7), the coefficients e_j can be determined as

$$e_j = \Omega(2j+1) \int_0^1 u(z) FR_j^{\Omega}(z) w(z) dz, \quad j = 0, 1, 2, \cdots. \tag{3.9}$$

For the practicality, considering the first $n+1$-terms of (3.8), we have

$$\begin{aligned} u(z) &\simeq \sum_{j=0}^{n} e_j FR_j^{\Omega}(z), \\ &= (\Lambda)^T \Psi(z), \end{aligned} \tag{3.10}$$

where

$$(\Lambda)^T = [e_0, e_1, \cdots, e_n],$$

and

$$\Psi(z) = [FR_0^{\Omega}(z), FR_1^{\Omega}(z), FR_2^{\Omega}(z), \cdots, FR_n^{\Omega}(z)]^T. \tag{3.11}$$

For $n = 4, \Omega = 1/2$, we have

$$\Psi(z) = \begin{pmatrix} 1 \\ 2\sqrt{z} - 1 \\ 6z - 6\sqrt{z} + 1 \\ 12\sqrt{z} - 30z + 20z^{\frac{3}{2}} - 1 \\ 90z + 70z^2 - 20\sqrt{z} - 140z^{\frac{3}{2}} + 1 \end{pmatrix},$$

and for $u(z) = 1 + z$, we have

$$(\Lambda)^T = \begin{pmatrix} \frac{4}{3} & \frac{1}{2} & \frac{1}{6} & 0 & 0 \end{pmatrix}.$$

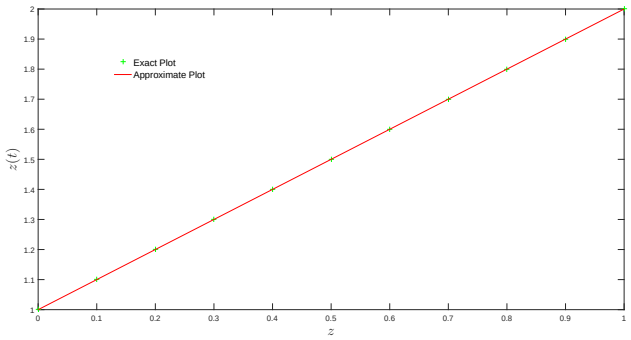

Figure 3. Exact and approximated graphs of the function $u(z) = 1 + z$ using FLFVs at $\Omega = 1/2$, and $n = 4$.

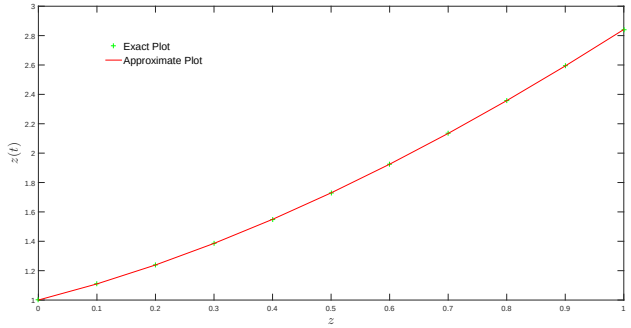

Figure 4. Exact and approximated graphs of the function $u(z) = \sin(z) + 1 + z^2$ using FLFVs at $\Omega = 1/2$, and $n = 4$..

4. Operational matrices of FLFVs

Operational matrices approach together with Spectral Tau approach is among of the approaches that has been frequently used to solve numerically the ordinary and partial FDEs (see [13–15, 19–22, 24–26]) and references therein. Under this approach, the numerical solutions are obtained by reducing the under study FDEs both ordinary and partial to an equivalent system of algebraic equations. The solution of the algebraic equations leads to the solution of the original FDEs. In recent, the authors in [19] extended the study of the generalized derivative operational matrix of CSLPs [13] to the generalized derivative operational matrix of orthogonal FLFVs in Caputo sense to solve numerically the multi-order FDEs. In this section, based on the study in [13, 19], we develop the new generalized integral operational matrix of orthogonal FLFVs in Riemann-Liouville sense.

Lemma 4.1. *The Caputo derivative of order $\beta > 0$ of FLFVs can be expressed as*

$$ {}_C\mathcal{D}^{\beta} FR_j^{\Omega}(z) = \sum_{q=0}^{j} a''_{(q,j)} \frac{\Gamma(q\Omega + 1)}{\Gamma(q\Omega - \beta + 1)} z^{q\Omega - \beta}, \tag{4.1} $$

where $a''_{(q,j)} = 0$ when $q\Omega \in \mathbb{R}_+$ and $q\Omega < \beta$. For other cases, $a''_{(q,j)} = a'_{(q,j)}$.

Proof. For the proof (see [19]). □

Lemma 4.2. *The Riemann Liouville integral of order $\alpha > 0$ of FLFVs can be expressed as*

$$ {}_{RL}J^{\alpha}FR_{j}^{\Omega}(z) = \sum_{q=0}^{j} a'_{(q,j)} \frac{\Gamma(q\Omega+1)}{\Gamma(q\Omega+\alpha+1)} z^{q\Omega+\alpha}. \tag{4.2} $$

Proof. Using linearity property and Eq (3.5), we have

$$ {}_{RL}J^{\alpha}FR_{j}^{\Omega}(z) = \sum_{q=0}^{j} a'_{(q,j)} RLJ^{\alpha} z^{q\Omega} \tag{4.3} $$

Now the lemma can be proved easily using ([27], Eq (22)). □

Lemma 4.3. *Suppose, $\Omega \in \mathbb{R}_+$, and $\alpha > 0$, then*

$$ \begin{aligned} &z^{\alpha+q\Omega} = \sum_{i=0}^{n} c'_{(r,i)} FR_{i}^{\Omega}(z), \\ &\text{where} \\ &c'_{(r,i)} = \Omega\,(2i+1) \sum_{r=0}^{i} \frac{(-1)^{(i+r)}\Gamma(i+r+1)}{\Gamma(i-r+1)(\Gamma(r+1))^2\Omega\,(q+1+r)+\alpha},\ i = 0, 1, \cdots, n. \end{aligned} \tag{4.4} $$

Proof. Using $(n+1)$ orthogonal FLFVs, we may approximate $z^{\beta+q\Omega}$, as

$$ z^{\alpha+q\Omega} \approx \sum_{i=0}^{n} c'_{(r,i)} FR_{i}^{\Omega}(z). \tag{4.5} $$

Using Eq (3.9), and after doing some lengthy calculations, we have

$$ c'_{(r,i)} = \Omega\,(2i+1) \sum_{r=0}^{i} \frac{(-1)^{(i+r)}\Gamma(i+r+1)}{\Gamma(i-r+1)(\Gamma(r+1))^2\Omega\,(q+1+r)+\alpha}. \tag{4.6} $$

Now using the Eqs (4.5) and (4.6), we can obtain the required result. □

Lemma 4.4. *Suppose, $\Omega \in \mathbb{R}_+$, and $\beta > 0$, then*

$$ \begin{aligned} &z^{q\Omega-\beta} = \sum_{i=0}^{n} c''_{(r,i)} FR_{i}^{\Omega}(z), \\ &\text{where} \\ &c''_{(i)} = \Omega\,(2i+1) \sum_{r=0}^{i} \frac{(-1)^{(i+r)}\Gamma(i+r+1)}{\Gamma(i-r+1)(\Gamma(r+1))^2\Omega\,(q+1+r)-\beta},\ i = 0, 1, \cdots, n. \end{aligned} \tag{4.7} $$

Proof. Using $(n+1)$ orthogonal FLFVs, we may approximate $z^{q\Omega-\beta}$, as

$$z^{q\Omega-\beta} \approx \sum_{i=0}^{n} c''_{(r,i)} FR_i^{\Omega}(z). \tag{4.8}$$

Using Eq (3.9), and after doing some lengthy calculations, we have

$$c''_{(i)} = \Omega\,(2i+1) \sum_{r=0}^{i} \frac{(-1)^{(i+r)}\Gamma(i+r+1)}{\Gamma(i-r+1)(\Gamma(r+1))^2\Omega\,(q+1+r)-\beta}. \tag{4.9}$$

Now using the Eqs (4.8) and (4.9), we can obtain the required result. □

4.1. The fractional integral and derivative operational matrices of FLFVs

In this section, the generalized operational matrices of fractional integral and fractional derivative for FLFVs in Riemann Liouville and Caputo senses are studied respectively.

Theorem 4.5. *Suppose $\Psi(z)$ be the orthogonal FLFVs as defined in* (3.11)*, and $\alpha > 0$ be the order of the integral consider in Riemann-Liouville sense, then*

$${}_{RL}J^{\alpha}\Psi(z) \approx \mathbf{D}^{\alpha}_{(n+1,n+1)}\Psi(z), \tag{4.10}$$

where $\mathbf{D}^{\alpha}$ is the $(n+1)\times(n+1)$ operational matrix which can be computed as

$$\mathbf{D}^{\alpha}_{(n+1,n+1)} = \sum_{q=0}^{j} \frac{a'_{(q,j)c'_{(r,i)}}\,\Gamma(q\Omega+1)}{(q\Omega+\alpha+1)},\ j=0,1,\cdots,n. \tag{4.11}$$

Proof. Using (3.11) and linearity of Riemann-Liouville fractional integral, we have

$${}_{RL}J^{\alpha}\Psi(z) = \sum_{q=0}^{j} a'_{(q,j)}{}_{RL}J^{\alpha}(z^{q\Omega}) \tag{4.12}$$

Using lemma (4.2), Eq (4.12) can be expressed as

$${}_{RL}J^{\alpha}\Psi(z) = \sum_{q=0}^{j} a'_{(q,j)} \frac{\Gamma(q\Omega+1)}{\Gamma(q\Omega+\alpha+1)} z^{\alpha+q\Omega}. \tag{4.13}$$

Now Eq (4.13) and Lemma 4.3 proves the required result. □

Remark 4.6. *The operational matrix of integration for CSLPs studied by Khan and Khalil [24] is a special case of Theorem 4.5 for $\Omega = 1$.*

Theorem 4.7. *Suppose $\Psi(z)$ be the orthogonal FLFVs as defined in* (3.11)*, and $\beta > 0$ be the order of the derivative consider in Caputo sense, then*

$${}_{C}\mathcal{D}^{\beta}\Psi(z) \approx \mathbf{Q}^{\beta}_{(n+1,n+1)}\Psi(z), \tag{4.14}$$

where $\mathbf{Q}^{\beta}$ is the $(n+1)\times(n+1)$ operational matrix which can be computed as

$$\mathbf{Q}^{\beta}_{(n+1,n+1)} = \sum_{q=\frac{\lceil\beta\rceil}{\Omega}}^{j} \frac{a'_{(q,j)c''_{(r,i)}}\,\Gamma(q\Omega+1)}{(q\Omega-\beta+1)},\ j=\frac{\lceil\beta\rceil}{\Omega},\frac{\lceil\beta\rceil}{\Omega}+1,\cdots. \tag{4.15}$$

Proof. Using (3.11) and linearity of Caputo fractional derivative, we have

$$ {}_C\mathcal{D}^{\beta}\Psi(z) = \sum_{q=0}^{j} a'_{(q,j)} C\mathcal{D}^{\beta}(z^{q\Omega}) \tag{4.16} $$

Using lemma (4.1), Eq (4.16) can be expressed as

$$ {}_C\mathcal{D}^{\beta}\Psi(z) = \sum_{q=\frac{\lceil\beta\rceil}{\Omega}}^{j} a'_{(q,j)} \frac{\Gamma(q\Omega+1)}{\Gamma(q\Omega-\beta+1)} z^{q\Omega-\beta}. \tag{4.17} $$

Now Eq (4.17) and lemma (4.4) proves the required result. □

Remark 4.8. *The operational matrix of derivatives for CSLPs studied by Saadatmandi and Dehghan [13] is a special case of Theorem 4.7 for* $\Omega = 1$.

5. Solution of multi-order FDEs

In this section, we are interested in the development of the computational algorithm to solve numerically the following generalized multi-order FDEs

$$ \begin{aligned} {}_C\mathcal{D}^{\alpha}u(z) &= g(z, u(z), {}_C\mathcal{D}^{\beta_1}u(z), {}_C\mathcal{D}^{\beta_2}u(z), \ldots, {}_C\mathcal{D}^{\beta_n}u(z)), \\ u^{(s)}(0) &= h_s, \ s = 0, 1, \ldots, n. \end{aligned} \tag{5.1} $$

where $n-1 < \alpha \le n$, $0 < \beta_1 < \beta_2 < \cdots < \beta_n < \alpha$, and ${}_C\mathcal{D}^{\alpha}$ is a Caputo derivative of order α defined in (2.2).

We are interested to approximate the solution in terms of orthogonal FLFVs, such that

$$ {}_C\mathcal{D}^{\alpha}u(z) = \Lambda^T\Psi(z). \tag{5.2} $$

Now integrating (5.2) in Riemann-Liouville sense and using the initial conditions $u^{(s)}(0) = h_s$, $s = 0, 1, \ldots, n$, we have

$$ u(z) = \Lambda^T J^{\alpha}\Psi(z) + \sum_{s=0}^{n} h_s z^s. \tag{5.3} $$

Using Theorem 4.5, Eq (5.3) can also be written as

$$ u(z) = \Lambda^T \mathbf{D}^{\alpha}_{(n+1,n+1)}\Psi(z) + \sum_{s=0}^{n} h_s z^s. \tag{5.4} $$

The terms in $\sum_{s=0}^{n} h_s z^s$ can also be approximated using FLFVs. So, Eq (5.4) can also be written as

$$ u(z) = \Lambda^T \mathbf{D}^{\alpha}_{(n+1,n+1)}\Psi(z) + H^T\Psi(z). \tag{5.5} $$

Now using Theorem 4.7 and Eq (5.5), the right hand side terms of Eq (5.1) can be approximated as

$$\begin{cases} {}_C\mathcal{D}^{\beta_0}u(z) = \Lambda^T \mathbf{D}^{\alpha}_{(n+1,n+1)} \mathbf{Q}^{\beta_0}_{(n+1,n+1)} \Psi(z) + H^T \mathbf{Q}^{\beta_0}_{(n+1,n+1)} \Psi(z), \\ {}_C\mathcal{D}^{\beta_1}u(z) = \Lambda^T \mathbf{D}^{\alpha}_{(n+1,n+1)} \mathbf{Q}^{\beta_1}_{(n+1,n+1)} \Psi(z) + H^T \mathbf{Q}^{\beta_1}_{(n+1,n+1)} \Psi(z), \\ \vdots \qquad\qquad \vdots \qquad\qquad \vdots \\ {}_C\mathcal{D}^{\beta_n}u(z) = \Lambda^T \mathbf{D}^{\alpha}_{(n+1,n+1)} \mathbf{Q}^{\beta_n}_{(n+1,n+1)} \Psi(z) + H^T \mathbf{Q}^{\beta_n}_{(n+1,n+1)} \Psi(z), \\ \text{and} \\ g(z) = G^T \Psi(z). \end{cases} \tag{5.6}$$

Now inserting (5.2) and (5.6) in (5.1), we have

$$\begin{aligned} \Lambda^T \Psi(z) &= \Lambda^T \mathbf{D}^{\alpha}_{(n+1,n+1)} \left(\mathbf{Q}^{\beta_0}_{(n+1,n+1)} + \mathbf{Q}^{\beta_1}_{(n+1,n+1)} + \cdots + \mathbf{Q}^{\beta_n}_{(n+1,n+1)} \right) \Psi(z) \\ &+ H^T \left(\mathbf{Q}^{\beta_0}_{(n+1,n+1)} + \mathbf{Q}^{\beta_1}_{(n+1,n+1)} + \cdots + \mathbf{Q}^{\beta_n}_{(n+1,n+1)} \right) \Psi(z) + G^T \Psi(z). \end{aligned}$$

After simplification, we have

$$\Lambda^T - \Lambda^T \mathbf{D}^{\alpha}_{(n+1,n+1)} \widehat{Q} - H^T \widehat{Q} - G^T, \tag{5.7}$$

where $\widehat{Q} = \left(\mathbf{Q}^{\beta_0}_{(n+1,n+1)} + \mathbf{Q}^{\beta_1}_{(n+1,n+1)} + \cdots + \mathbf{Q}^{\beta_n}_{(n+1,n+1)} \right)$.

Equation (5.7) is a matrix equation of Sylvester type that can be easily solved for the unknown Λ^T using any computational software. By inserting the values of Λ^T in Eq (5.5), we get the approximate solution of (5.1).

6. Test Examples

In this section, the applicability of the method is studied by solving various examples and comparing their analytical solutions with the approximate solutions obtained using our developed computational numerical algorithm.

Example 1. We consider the following non-homogeneous Bagley-Torvik equation [13, 19, 28]

$${}_C\mathcal{D}^2 u(z) +_C \mathcal{D}^{\frac{3}{2}} u(z) + u(z) = 1 + z, \tag{6.1}$$

subject to the following initial conditions

$$u(0) = 1 = u'(0). \tag{6.2}$$

The exact solution is given as under

$$u(z) = 1 + z. \tag{6.3}$$

Here, we have

$$G^T = \left[\frac{3}{2}, \frac{1}{2}, 0 \right], \quad H^T = \left[\frac{3}{2}, \frac{1}{2}, 0 \right], \quad \Lambda^T = [0, 0, 0]. \tag{6.4}$$

and

$$\mathbf{Q}^{\frac{3}{2}} = \begin{bmatrix} 0 & 0 & 0 \\ 0 & 0 & 0 \\ 9.0270 & 5.4162 & -1.2896 \end{bmatrix}, \mathbf{D}^2 = \begin{bmatrix} 0.1667 & 0.2500 & 0.0833 \\ -0.0833 & -0.1000 & 0 \\ 0.0167 & 0 & -0.0238 \end{bmatrix}. \tag{6.5}$$

Using (6.4) and (6.5) in (5.5), we get the exact solution of the problem (6.1)–(6.2).

Remark 6.1. *The results of Example 1 at various values of n obtained by using our method are compared with the results obtained by using the method [4] at n* = 10 *in Tables 1–4 and Figure 5. We observe that at various values of n (the number of terms of FLFVs), the exact solution and the approximate solution obtained by using our method coincide, (see Table 2 and Figure 5). However, the results obtained by using the method in [4] yield less accurate results, (see Table 2–4 and Figure 5).*

Table 1. Comparison of the approximate solution (AS) for Example 1 obtained by using our proposed method (PM) with the AS obtained by using the method ([4], Example 2).

z	Exact Solution	AS using PM at $n = 2$	AS in [4] at $n = 10$ (number of neurons)
0	1.00	1.00	1.024862
0.1	1.10	1.10	1.121206
0.2	1.20	1.20	1.220821
0.3	1.30	1.30	1.323041
0.4	1.40	1.40	1.426952
0.5	1.50	1.50	1.531330
0.6	1.60	1.60	1.634569
0.7	1.70	1.70	1.734591
0.8	1.80	1.80	1.828738
0.9	1.90	1.90	1.913640
1.0	2.00	2.00	1.985057

Table 2. Comparison of the Absolute errors for Example 1 obtained by using our proposed method (PM) at $n = 2$ (number of terms of FLFVs) with the absolute errors obtained by using the method ([4], Example 2) at $n = 10$ (number of neurons).

z	Absolute error using [4]	Absolute error using PM
0	$2.30e-2$	0
0.1	$2.69e-2$	0
0.2	$3.13e-2$	0
0.3	$3.45e-2$	0
0.4	$3.45e-2$	0
0.5	$2.87e-2$	0
0.6	$1.36e-2$	0
0.7	$1.49e-2$	0
0.8	$2.30e-2$	0
0.9	$2.69e-2$	0
1.0	$3.13e-2$	0

Table 3. Comparison of the Absolute errors for Example 1 obtained by using our proposed method (PM) at $n = 8$ (number of terms of FLFVs) with the absolute errors obtained by using the method ([4], Example 2) at $n = 10$ (number of neurons).

z	Absolute error using [4]	Absolute error using PM
0	$2.30e-2$	0
0.1	$2.69e-2$	0
0.2	$3.13e-2$	0
0.3	$3.45e-2$	0
0.4	$3.45e-2$	0
0.5	$2.87e-2$	0
0.6	$1.36e-2$	0
0.7	$1.49e-2$	0
0.8	$2.30e-2$	0
0.9	$2.69e-2$	0
1.0	$3.13e-2$	0

Table 4. Comparison of the Absolute errors for Example 1 obtained by using our proposed method (PM) at $n = 10$ (number of terms of FLFVs) with the absolute errors obtained by using the method ([4], Example 2) at $n = 10$ (number of neurons).

z	Absolute error using [4]	Absolute error using PM
0	$2.30e-2$	0
0.1	$2.69e-2$	0
0.2	$3.13e-2$	0
0.3	$3.45e-2$	0
0.4	$3.45e-2$	0
0.5	$2.87e-2$	0
0.6	$1.36e-2$	0
0.7	$1.49e-2$	0
0.8	$2.30e-2$	0
0.9	$2.69e-2$	0
1.0	$3.13e-2$	0

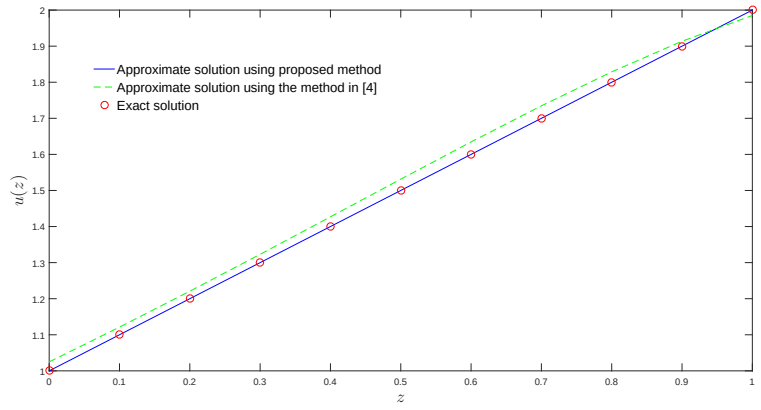

Figure 5. Comparison of the approximate solution of Example 1 obtained using the proposed method at $n = 2$ with the approximate solution obtained using the method of [4] at $n = 10$.

Remark 6.2. *In Tables 5 and 6, the results of Example 1 obtained by using our method are compared with the results obtained by using the methods in [5] and [6]. Our proposed method provides the exact solution at n = 2 (first three terms of FLFVs). However, the methods in [5] and [6] provide the exact solution at n = 6 (first seven terms of Taylor series, and first seven terms of Bessel series). This shows that our proposed method is numerically more efficient.*

Table 5. Comparison of the approximate solution (AS) for Example 1 obtained by using our proposed method (PM) with the AS obtained by using the method ([5], Example 1).

z	Exact solution	AS using PM at $n = 2$	AS in [5] at $n = 6$ (number of terms of Taylor series)
0	1.00	1.00	1.00
0.1	1.10	1.10	1.10
0.2	1.20	1.20	1.20
0.3	1.30	1.30	1.30
0.4	1.40	1.40	1.40
0.5	1.50	1.50	1.50
0.6	1.60	1.60	1.60
0.7	1.70	1.70	1.70
0.8	1.80	1.80	1.80
0.9	1.90	1.90	1.90
1.0	2.00	2.00	2.00

Table 6. Comparison of the approximate solution (AS) for Example 1 obtained by using our proposed method (PM) with the AS obtained by using the method ([6], Example 1).

z	Exact solution	AS using PM at $n = 2$	AS in [6] at $n = 6$ (number of terms of Bessel series)
0	1.00	1.00	1.00
0.1	1.10	1.10	1.10
0.2	1.20	1.20	1.20
0.3	1.30	1.30	1.30
0.4	1.40	1.40	1.40
0.5	1.50	1.50	1.50
0.6	1.60	1.60	1.60
0.7	1.70	1.70	1.70
0.8	1.80	1.80	1.80
0.9	1.90	1.90	1.90
1.0	2.00	2.00	2.00

Example 2. Consider the following non-homogeneous multi-order fractional problem [21, 32]

$$\begin{aligned} {}_C\mathcal{D}^{\alpha}u(z) &= a_C\mathcal{D}^{\beta_0}u(z) + b_C\mathcal{D}^{\beta_1}u(z) + c_C\mathcal{D}^{\beta_2}u(z) \\ &+ d_C\mathcal{D}^{\beta_3}u(z) + G(z),\ z \in [0,1],\ \ 0 < \alpha < 2, \end{aligned} \tag{6.6}$$

subject to the following initial conditions

$$u(0) = 0,\ \ u'(0) = 0. \tag{6.7}$$

The source term is as under

$$G(z) = 4\,z - z^2 - \frac{6776\,z^{\frac{3}{2}}}{4503} + 42\,z^5 - 14\,z^6 + z^7 + \frac{1516\,z^{\frac{13}{2}}}{5629} - 2.$$

The exact solution corresponding to $\alpha = 2, a = c = -1, b = 2, d = 0, \beta_0 = 0, \beta_1 = 1, \beta_2 = \frac{1}{2}$ is given below

$$u(z) = z^7 - z^2.$$

We study the Example 2 by comparing the approximate results obtained using our algorithm with the approximate results achieved using the methods in [21, 32]. We observe that our method produces better approximate results and higher precision in the approximate solution, see Table 7, Figure 6–9.

The applicability of the numerical algorithm is tested at various scale levels. We observe that with the increase in scale level, the approximate solution and the exact solution have great resemblance, see Figure 7. Also, at $n = 7$, the approximate solution is equal to the exact solution, $u(z) = z^7 - z^2$ of the problem (6.6)–(6.7), see Table (7, Column 7]. We also calculate the amount of the absolute errors at scale level, $n = 4, 6, 7$. we analyze that with the increase in scale level, the amount of the absolute errors decreases significantly, see Table 7 and Figure 9. It is worth to mention that by taking few terms of orthogonal FLFVs, the good match is obtained between the approximate solution and the exact solution. For example compare the results of ([21], Figures 4–5 and Table 1) and ([32], Figure 2) with the results of our paper (Figures 6–8 and Table (7, Column 7).

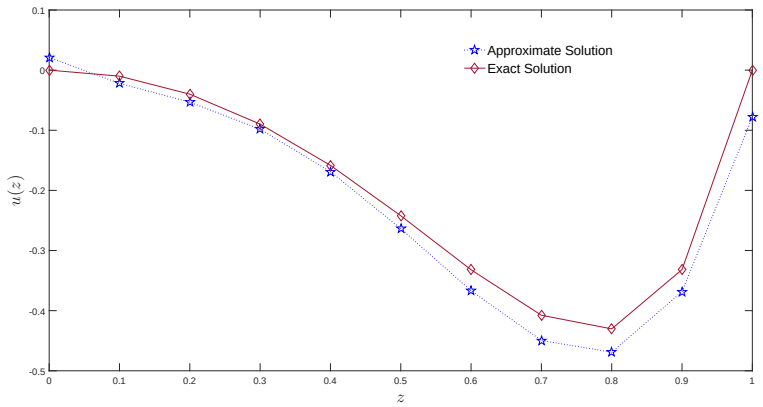

Figure 6. Graphs of exact solution and approximate solution of Example 2 at $\Omega = 1, \alpha = 2$ and $n = 4$.

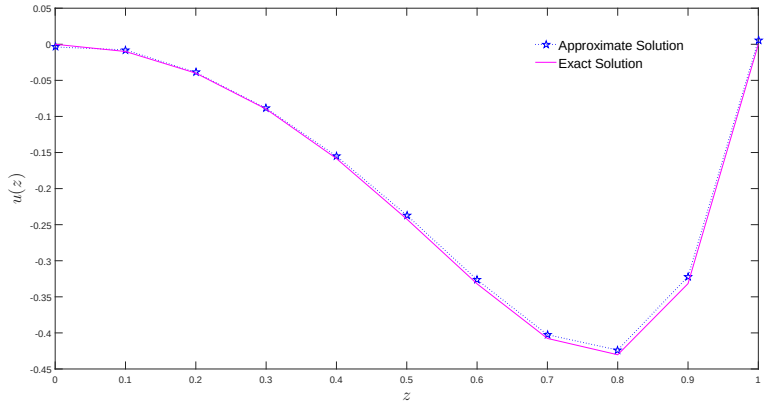

Figure 7. Graphs of exact solution and approximate solution of Example 2 at $\Omega = 1, \alpha = 2$ and $n = 5$.

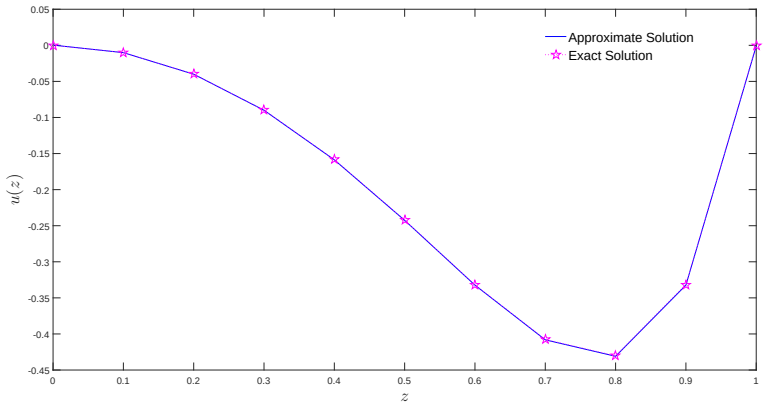

Figure 8. Graphs of exact solution and approximate solution of Example 2 at $\Omega = 1, \alpha = 2$ and $n = 6$.

Table 7. Comparison of absolute error of Example 2 computed using our proposed method (PM) and the absolute error computed with [21] at $n = 4, 6, 7$.

z	$n = 4$ [21]	$n = 4$ PM	$n = 6$ [21]	$n = 6$ PM	$n = 7$ [21]	$n = 7$ PM
0.2	0.0844	0.0132	0.0044	0.00003	2.81025203108243e-15	0
0.4	0.3501	0.0105	0.0079	0.00035	6.63358257213531e-15	0
0.6	0.6734	0.0349	0.0143	0.00034	3.27515792264421e-15	0
0.8	1.0234	0.0387	0.0214	0.00069	4.25770529943748e-14	0
1	1.6700	0.0780	0.0280	0.00103	2.43819897540083e-13	0

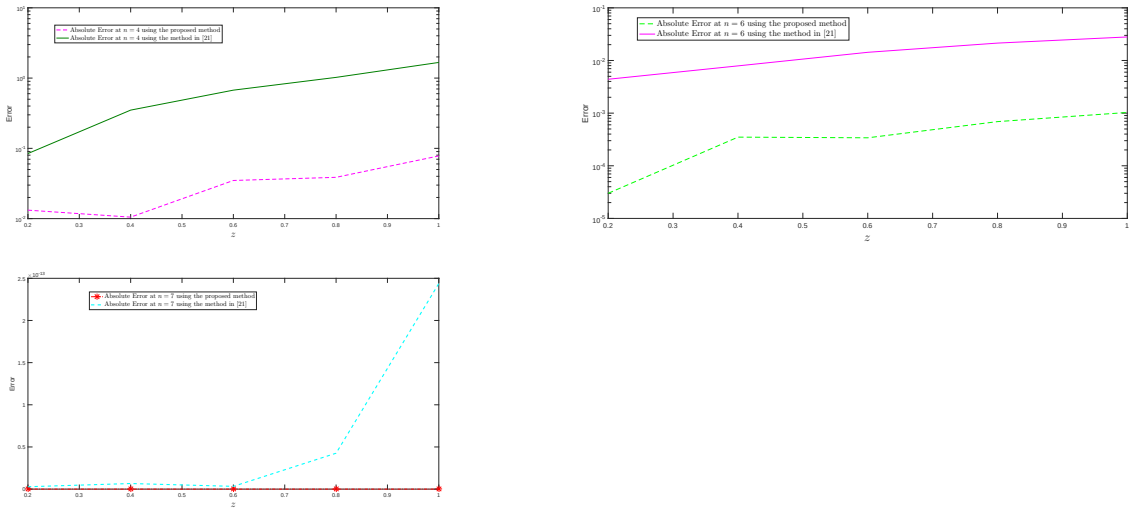

Figure 9. Comparison of the error plots of Example 2 with the results of [21] at $n = 4, 6, 7$.

Example 3. Consider the following non-homogeneous multi-order fractional problem [21]

$$\begin{aligned} {}_C\mathcal{D}^{\alpha}u(z) &= a_C\mathcal{D}^{\beta_0}u(z) + b_C\mathcal{D}^{\beta_1}u(z) + c_C\mathcal{D}^{\beta_2}u(z) \\ &+ d_C\mathcal{D}^{\beta_3}u(z) + G(z),\ z \in [0,1],\ \ 0 < \alpha < 2, \end{aligned} \tag{6.8}$$

subject to the following initial conditions

$$u(0) = 0,\ \ u'(0) = 0. \tag{6.9}$$

The source term is as under

$$G(z) = 6z + z^3 - \frac{12}{\Gamma(\frac{7}{3})}z^{\frac{4}{3}} + \frac{6}{\Gamma(\frac{10}{3})}z^{\frac{7}{3}}.$$

The exact solution corresponding to $\alpha = 2, a = c = -1, b = 0, d = 2, \beta_0 = 0, \beta_2 = \frac{2}{3} \in (0,1)$, and $\beta_3 = \frac{5}{3} \in (1,2)$ is given below

$$u(z) = z^3.$$

Here for $n = 3$, we have

$$\begin{cases} G^T = \begin{bmatrix} -0.4215 & -0.6867 & 0.0216 & 0.1984 \end{bmatrix}, \\ H^T = \begin{bmatrix} 0 & 0 & 0 & 0 \end{bmatrix}, \\ \Lambda^T = \begin{bmatrix} 2.9991 & 3.0000 & 0.0000 & -0.0000 \end{bmatrix}. \end{cases} \tag{6.10}$$

and

$$\begin{cases} \mathbf{Q}^{\frac{2}{3}} = \begin{bmatrix} 0 & 0 & 0 & 0 \\ 1.6796 & 0.7199 & -0.2391 & 0.1292 \\ -0.7199 & 3.0236 & 1.3844 & -0.5039 \\ 1.4398 & -0.6645 & 3.9594 & 1.9994 \end{bmatrix}, \\ \mathbf{Q}^{\frac{5}{3}} = \begin{bmatrix} 0 & 0 & 0 & 0 \\ 0 & 0 & 0 & 0 \\ 10.0786 & 4.3194 & -1.4398 & 0.7753 \\ -7.1990 & 30.2358 & 13.8442 & -5.0393 \end{bmatrix}, \\ \mathbf{D}^2 = \begin{bmatrix} 0.1667 & 0.2500 & 0.0833 & 0 \\ -0.0833 & -0.1000 & 0 & 0.0167 \\ 0.0167 & 0 & -0.0238 & 0 \\ 0 & 0.0071 & 0 & -0.0111 \end{bmatrix}. \end{cases} \tag{6.11}$$

Using (6.10) and (6.11) in (5.5), we get the exact solution, $u(z) = z^3$ of the problem (6.8) and (6.9).

We study the Example 3 by comparing the approximate results obtained using our algorithm with the approximate results achieved using the methods in [21]. We observe that our method produces better approximate results and higher precision in the approximate solution, see Table 8, Figures 10 and 11.

We observe that by increasing the scale level, the absolute error amount decreases significantly, see Table 8. Also at low scale level, $n = 3$, the exact solution of the problem, (6.8)–(6.9) is obtained which shows that our proposed algorithm is more efficient as compared to [21], see Figures 10 and 11 and Table 8.

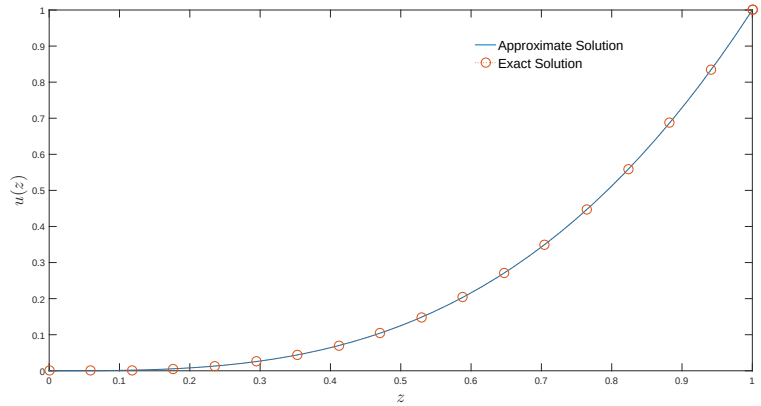

Figure 10. Graphs of exact solution and approximate solution of Example 3 at $\Omega = 1, \alpha = 2$ and $n = 3$.

Table 8. Comparison of absolute error of Example 3 computed using our proposed method (PM) and the absolute error computed with [21] at $n = 2, 3$.

z	Exact solution	$n = 2$ [21]	$n = 2$ PM	$n = 3$ [21]	$n = 3$ PM
0.2	0.0080	0.0614	0.0291	2.55004350968591e-16	0
0.4	0.0640	0.1541	0.0885	2.77555756156289e-16	0
0.6	0.2160	0.3339	0.1239	3.33066907387547e-16	0
0.8	0.5120	0.6488	0.0875	4.44089209850063e-16	0
1	1.0000	1.1468	0.0689	6.66133814775094e-16	0

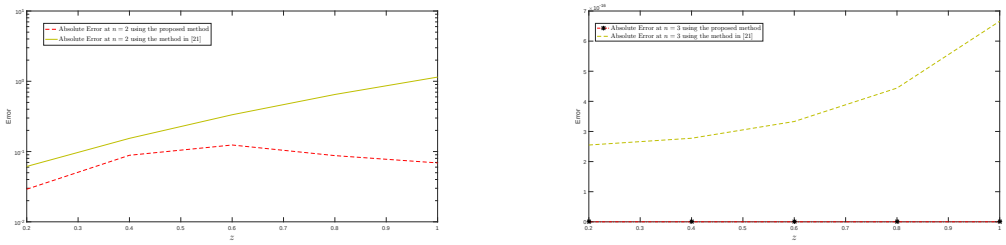

Figure 11. Comparison of the error plots of Example 3 with the results of [21] at $n = 2, 3$.

Example 4. Consider the following fractional problem [19, 30]

$$ {}_C\mathcal{D}^{\alpha}u(z) = -u(z) + G(z),\ z \in [0, 1],\ 0 < \alpha \leq 1, \tag{6.12} $$

subject to the following initial condition

$$ u(0) = 0. \tag{6.13} $$

The source term is as under

$$ G(z) = \frac{2z^{2-\alpha}}{\Gamma(3-\alpha)} - \frac{z^{1-\alpha}}{\Gamma(2-\alpha)} + z^2 - z. $$

The exact solution of the problem (6.12)–(6.13) is as under

$$ u(z) = z^2 - z. $$

We study the Example 4 to investigate the applicability of orthogonal FLFVs at various fractional values of Ω, and α, see Figures 12–14. We observe that at various choices of $\alpha = 0.5, 0.7, 0.9$, and $\Omega = \frac{1}{2}, \frac{1}{3}$, the approximate results have a great compatibility with the exact solution. Also at $n = 2(r+1)$, the exact solution of the problem (6.12)–(6.13) can be obtained for $\Omega = \frac{1}{r+1} > \frac{\alpha}{2},\ \ r \in \mathbb{N}$. For instance, by inserting (6.14) in (5.5), we can obtain the exact solution, $u(z) = z^2 - z$ of (6.12)–(6.13), see Figure 14.

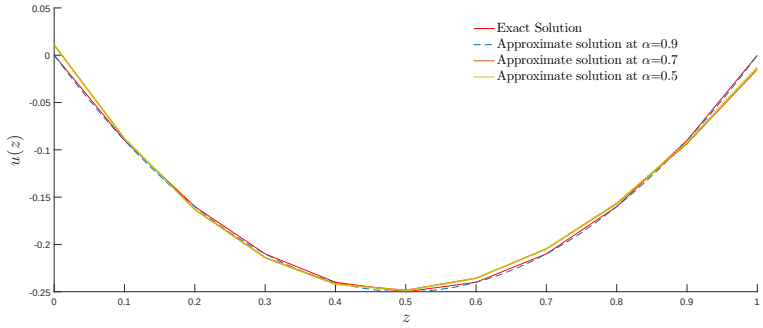

Figure 12. Graphs of exact solution and approximate solution of Example 4 at $\Omega = \frac{1}{3}, n = 4$, and various values of α.

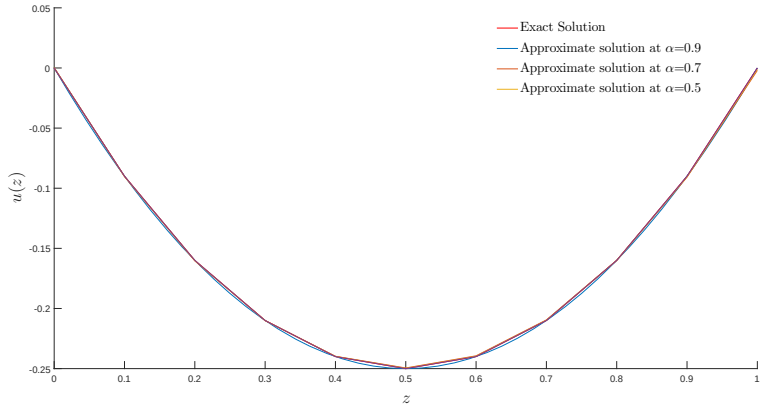

Figure 13. Graphs of exact solution and approximate solution of Example 4 at $\Omega = \frac{1}{2}, n = 4$, and various values of α.

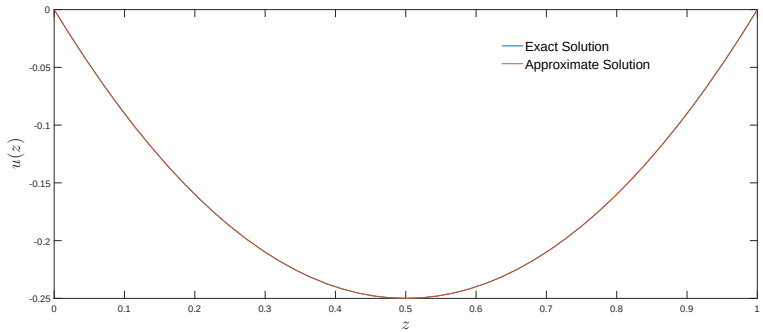

Figure 14. Graphs of exact solution and approximate solution of Example 4 at $\Omega = \alpha = \frac{1}{2}, n = 4$.

Here for $n = 4, \Omega = \frac{1}{2}$, and $\alpha = \frac{1}{2}$, we have

$$\begin{cases} \Psi(z) = \begin{bmatrix} 1 \\ 2\sqrt{z} - 1 \\ 6z - 6\sqrt{z} + 1 \\ 12\sqrt{z} - 30z + 20z^{\frac{3}{2}} - 1 \\ 90z + 70z^2 - 20\sqrt{z} - 140z^{\frac{3}{2}} + 1 \end{bmatrix}, \\ \mathbf{D}^{1/2} = \begin{bmatrix} 0.5642 & 0.5642 & 0 & 0 & 0 \\ 0.0266 & 0.3220 & 0.2954 & 0 & 0 \\ -0.0799 & -0.0634 & 0.2421 & 0.2257 & 0 \\ -0.00249 & -0.0849 & -0.0713 & 0.2001 & 0.1899 \\ -0.0080 & -0.0083 & -0.0777 & -0.0694 & 0.1752 \end{bmatrix}, \\ G^T = \begin{bmatrix} -\frac{47997861414693660616975379209 94}{14934156798733865782131057530655} \\ \frac{38344692221904871836977163678 1}{29868313597467731564262115061310} & \frac{1111693540705723}{2245056328819542} & \frac{655651031513913}{3741760548032570} & \frac{1}{70} \end{bmatrix}, \\ \Big[\Lambda^T = -0.18806 \quad 0.1128 \quad 0.3761 \quad 0.0752 \quad -0.0000\Big]. \end{cases} \tag{6.14}$$

Example 5. Consider the following fractional problem [19, 31]

$$ {}_C\mathcal{D}^{\alpha} u(z) - u(z) = 1, \ z \in [0, 1], \ 0 < \alpha \leq 1, \tag{6.15}$$

subject to the following initial condition

$$u(0) = 0. \tag{6.16}$$

The exact solution of the problem (6.15)–(6.16) is as under

$$u(z) = \sum_{j=1}^{\infty} \frac{z^{\alpha j}}{\Gamma(\alpha j + 1)}.$$

We study the Example 5 to investigate the applicability of orthogonal FLFVs at various fractional values of Ω, and α, see Figures 15 and 16. We observe that for various choices of $\Omega = 0.4, 0.6, 0.8, 1$, and $\alpha = 0.9$, there is a good compatibility between the exact solution and the approximate solution. Also, we get improve approximate results with the increase in scale level, see Figure 16. We also determine the amount of the absolute error at scale level, $n = 10$ and for various choices of Ω to investigate the efficiency and accuracy of the proposed algorithm for fractional choices of Ω, see Table 9. We also analyze the effect of the fractional parameter, α by comparing the approximate solution with the exact solution, see Figure 17.

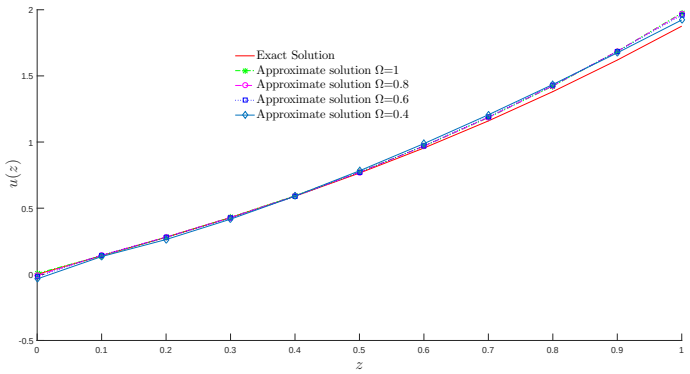

Figure 15. Graphs of exact solution and approximate solution of Example 5 at $\alpha = 0.9, n = 3$ and various choices of Ω.

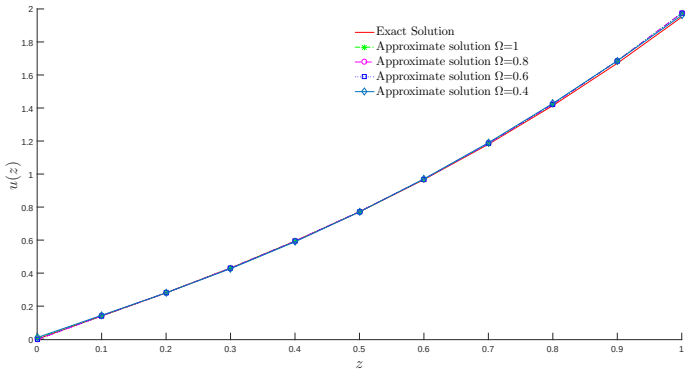

Figure 16. Graphs of exact solution and approximate solution of Example 5 at $\alpha = 0.9, n = 4$ and various choices of Ω.

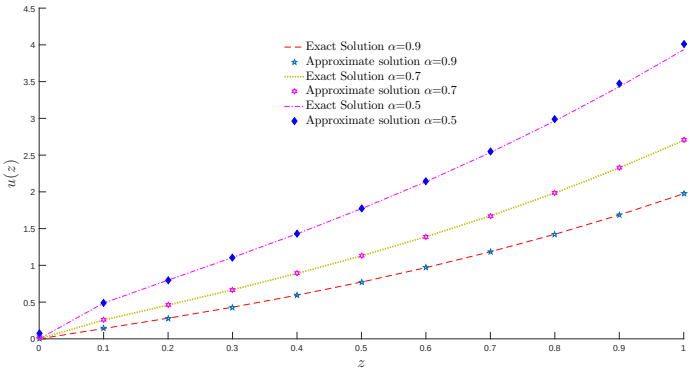

Figure 17. Graphs of exact solution and approximate solution of Example 5 at $n = 7, \Omega = 1$ and various choices of α.

Table 9. Absolute error of Example 5 at $n = 10$ and various choices of $\Omega = \alpha$.

z	$\Omega = \alpha = \frac{3}{4}$	$\Omega = \alpha = \frac{1}{2}$	$\Omega = \alpha = \frac{2}{3}$
0.2	4.273327e-11	5.870078e-07	9.236112e-10
0.4	8.335039e-09	2.999352e-05	1.401714e-07
0.6	2.455070e-07	3.010034e-04	2.873981e-06
0.8	2.731391e-06	1.568348e-03	2.478263e-05
1	1.782081e-05	5.703710e-03	1.328454e-04

Example 6. Consider the following fractional problem [13]

$$ {}_C\mathcal{D}^{\alpha}u(z) = -u(z),\ z \in [0,1],\ \ 0 < \alpha \leq 2, \tag{6.17} $$

subject to the following initial conditions

$$ u(0) = 1,\ \ u'(0) = 0. \tag{6.18} $$

The condition, $u'(0) = 0$ is applicable only when $\alpha > 1$.
The exact solution of the problem (6.17)–(6.18) is as under

$$ u(z) = \sum_{j=0}^{\infty} \frac{(-z^{\alpha})^j}{\Gamma(\alpha j + 1)}. $$

We study Example 6 to check the applicability of our proposed technique when $0 < \alpha < 1$, and $1 < \alpha < 2$, see Figures 18–23, Tables 10 and 11. We also investigate the accuracy and validity of the FLFVs for various choices of $\alpha = \Omega$, see Tables 10 and 11. We also observe the effect of the fractional parameter α by comparing the exact solution with the approximate solution, see Figures 21 and 22. We observe that with the increase in scale level n and $\alpha \longrightarrow 2$, the approximate solution of the problem (6.17)–(6.18) approaches to the solution of classical order differential equation, see Figures 21 and 22. We also observe that when $0 < \alpha < 1$ then at very low scale level $n = 2, 3$, the approximate solution shows great resemblance with the exact solution, see Figures 18–19. We also determine the absolute errors at scale level $n = 10$, and for various choices of $\alpha = \Omega$. We observe that our technique is more efficient as compared to the method used in [13], see Table 11 and Figure 23.

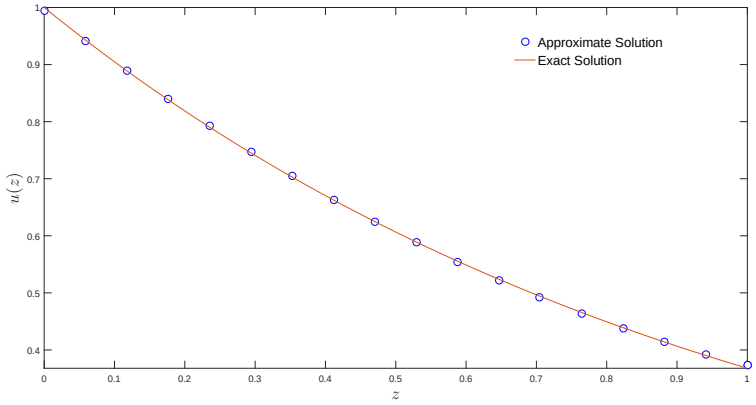

Figure 18. Graphs of exact solution and approximate solution of Example 6 at $\Omega = 1, \alpha = 1$ and $n = 2$.

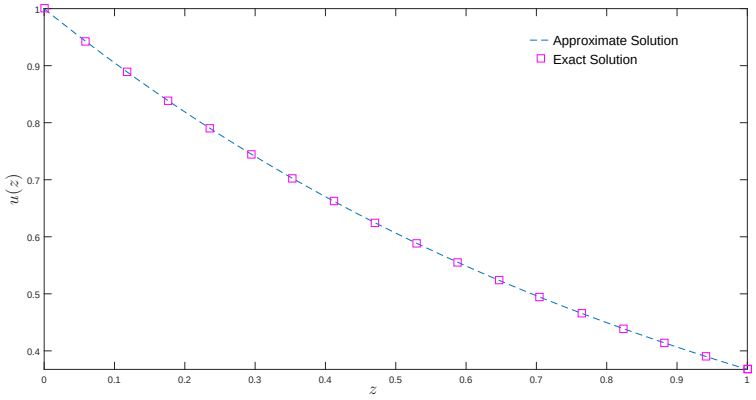

Figure 19. Graphs of exact solution and approximate solution of Example 6 at $\Omega = 1, \alpha = 1$ and $n = 3$.

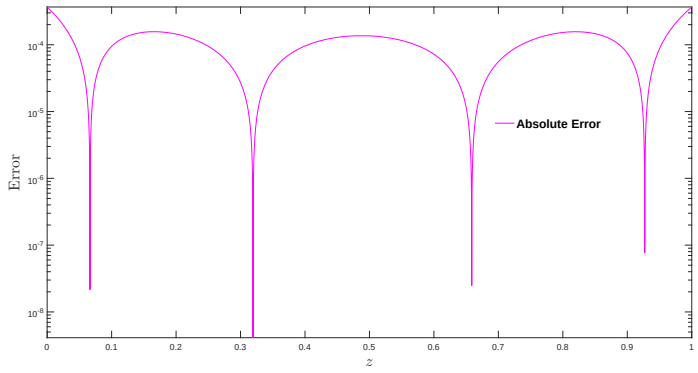

Figure 20. Error plot of Example 6 at $\Omega = 1, \alpha = 1$ and $n = 3$.

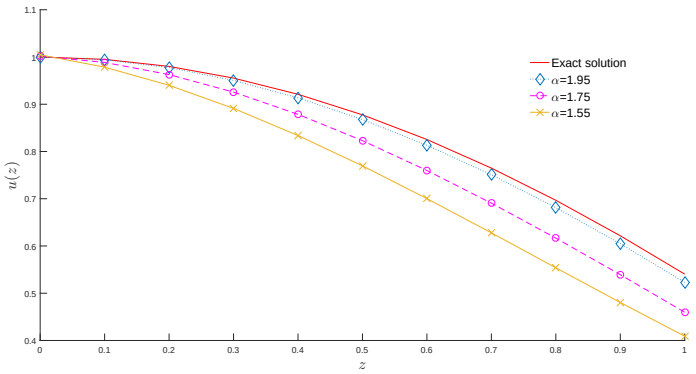

Figure 21. Graphs of exact solution and approximate solution of Example 6 at $\Omega = 1, n = 3$, and various values of α.

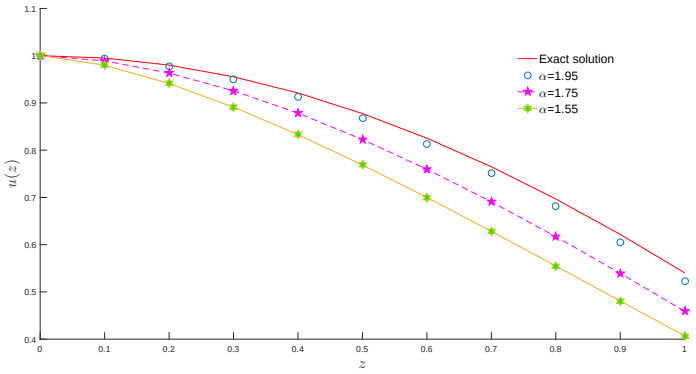

Figure 22. Graphs of exact solution and approximate solution of Example 6 at $\Omega = 0.95, n = 4$, and various values of α.

Table 10. Absolute error of Example 6 at $n = 10$ and various choices of $\Omega = \alpha$.

z	$\Omega = \alpha = \frac{1}{2}$	$\Omega = \alpha = \frac{3}{4}$	$\Omega = \alpha = \frac{2}{3}$	$\Omega = \alpha = \frac{5}{4}$	$\Omega = \alpha = \frac{7}{4}$	$\Omega = \alpha = \frac{3}{2}$
0.2	4.212086e-07	2.509733e-11	6.980854e-10	8.742474e-17	2.671553e-18	1.176754e-17
0.4	1.792713e-05	6.879759e-09	1.070398e-07	4.165262e-16	9.565113e-19	1.463810e-16
0.6	1.593986e-04	1.891806e-07	2.018518e-06	2.007704e-14	3.257643e-18	3.281789e-16
0.8	7.478411e-04	1.975211e-06	1.612752e-05	1.013113e-12	4.161064e-18	7.977363e-16
1	2.473455e-03	1.213707e-05	8.053908e-05	2.159538e-11	2.954844e-17	1.218018e-14

Table 11. Comparison of absolute error of Example 6 computed using our proposed method (PM) with the absolute error computed using [13] at $n = 10, \Omega = 1$ and at various choices of α.

α	$z = 0.1$	$z = 0.1PM$	$z = 0.3$	$z = 0.3PM$	$z = 0.5$	$z = 0.5PM$	$z = 0.7$	$z = 0.7PM$	$z = 0.9$	$z = 0.9PM$
1.2	3.1e-03	2.2e-05	2.8e-03	1.9e-05	4.5e-03	1.2e-05	3.6e-03	1.6e-05	1.8e-03	2.0e-05
1.4	1.0e-03	1.6e-05	7.0e-04	1.4e-05	1.3e-03	7.9e-06	1.1e-03	1.1e-05	2.4e-04	1.4e-05
1.6	3.0e-04	7.5e-06	1.3e-04	6.3e-06	3.1e-04	3.4e-06	3.0e-04	4.9e-06	6.2e-07	6.1e-06
1.8	6.1e-05	2.2e-06	1.4e-05	1.8e-06	4.9e-05	9.2e-07	5.3e-05	1.4e-06	8.8e-06	1.7e-06
0.2	2.9e-01	2.3e-03	4.5e-01	1.9e-02	7.4e-01	5.3e-02	3.7e-01	1.0e-01	2.0e-01	1.8e-01
0.4	3.9e-01	7.0e-04	5.1e-01	1.0e-03	7.3e-01	1.5e-03	3.3e-01	2.4e-03	2.2e-01	8.2e-03
0.6	6.7e-03	3.8e-04	2.0e-05	4.4e-04	5.2e-03	3.32e-04	4.4e-03	3.42e-04	4.6e-03	3.41e-04
0.8	1.1e-03	1.1e-04	2.1e-04	1.14e-04	8.4e-04	7.8e-05	8.7e-04	9.5e-05	5.8e-04	1.2e-04

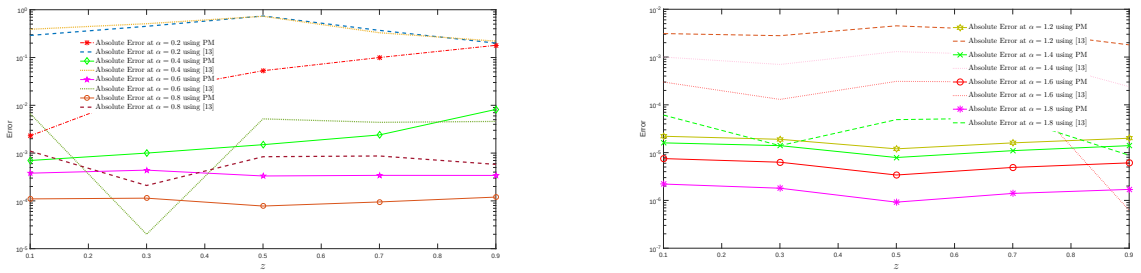

$0 < \alpha < 1.$ $1 < \alpha < 2.$

Figure 23. Comparison of the error plots of Example 6 with the results of [13] at $n = 10$, $0 < \alpha < 2$ and $\Omega = 1$.

7. Conclusions

We proposed a numerical method which is completely based on the fractional derivative and integral operational matrices of FLFVs. The proposed method is independent of the choice of the suitable collocation points and expansion of the residual function as a series of orthogonal polynomials. Consequently, the proposed method produced high efficient numerical results as compared to the Spectral tau method [13], Bessel collocation method [6], Taylor matrix method [5], function approximation theory [21], and stochastic technique [4]. The other novel aspect of our article is the development of new integral and derivative operational matrices in Riemann-Liouville and Caputo senses respectively. As an applications of the proposed method, we solved various MOFDEs corresponding to initial conditions. Our approach has ability to reduce the MOFDEs into a system of Sylvester types matrix equations which can be solved using *MATLAB* built in function *lyap*(.). The proposed results are not sufficient to solve numerically the fractional boundary value problems (BVPs). We are interested in extending the developed numerical results for fractional BVPs as well to partial FDEs by developing some more operational matrices.

Acknowledgments

We are grateful to the reviewers for their comments and suggestions which improve the quality of article. The research is supported by Cankaya University, Department of Mathematics, Turkey.

Conflict of interest

The authors declare no conflict of interest.

References

1. E. Ahmed, A. Elgazzar, On fractional order differential equations model for non-local epidemics, *Phys. A.,* **15** (2007), 607–614.
2. W. Chen, A speculative study of $\frac{2}{3}$-order fractional Laplacian modeling of turbulence: Some thoughts and conjectures, *Chaos*, **16** (2006), doi: 10.1063/1.2208452.
3. W. Chen, H. Sun, X. Zhang, D. Korosak, Anomalous diffusion modeling by fractal and fractional derivatives, *Comput. Math. Appl.,* **59** (2010), 1754–1758.
4. M. A. Z. Raja, J. A. Khan, I. M. Qureshi, Solution of fractional order system of Bagley-Torvik equation using evolutionary computational Iintelligence, *Math. Probl. Eng.,* (2011), doi:10.1155/2011/675075.
5. M. Gülsu, Y. Oztürk, A. Anapali, Numerical solution of the fractional Bagley-Torvik equation arising in fluid mechanics, *Int. J. Comput. Math.,* (2015), doi: 10.1080/00207160.2015.1099633.
6. S. Yüzbaşi, Numerical solution of the Bagley-Torvik equation by the Bessel collocation method, *Math. Meth. Appl. Sci.,* (2012), doi: 10.1002/mma.2588.
7. H. Sun, D. Chen, Y. Zhang, L. Chen, Understanding partial bed-load transport: Experiments and stochastic model analysis, *J. Hydrol.*, **521** (2015), 196–204.
8. H. Sun, W. Chen, Y. Chen, Variable-order fractional differential operators in anomalous diffusion modeling, *Phys. A.,* **388** (2009), 4586–4592.
9. Y. Rossikhin, M. Shitikova, Application of fractional derivatives to the analysis of damped vibrations of viscoelastic single mass systems, *Acta Mech.,* **120** (1997), 109–125.
10. A. A. Kilbas, H. M. Srivastava, J. J. Trujillo, *Theory and Application of Fractional Differential Equations*, New York, NY, USA, Elsevier Science B.V., 2006.
11. R. El Attar, *Special Functions and Orthogonal Polynomials*, New York, Lulu Press, 2006.
12. I. Podlubny, *Fractional Differential equations*, New York, Academic Press, 1998.
13. A. Saadatmandi, M. Dehghan, A new operational matrix for solving fractional-order differential equations, *Comput. Math. Appl.,* **59** (2010), 1326–1336.
14. E. H. Doha, A. H. Bhrawy, S. S. Ezz-Eldien, A Chebyshev spectral method based on operational matrix for initial and boundary value problems of fractional order, *Comput. Math. Appl.*, **62** (2011), 2364–2373.

15. M. H. Atabakzadeh, M. H. Akrami, G. H. Erjaee, Chebyshev Operational Matrix Method for Solving Multi-order Fractional Ordinary Differential Equations, *Appl. Math. Model.,* **37** (2013), 8903–8911.

16. E. H. Doha, A. H. Bhrawy, S. S. Ezz-Eldien, Efficient Chebyshev spectral methods for solving multi-term fractional orders differential equations, *Appl. Math. Model.,* **35** (2011), 5662–5672.

17. H. Zhang, X. Jiang, F. Zeng, G. Em Karniadakis, A stabilized semi-implicit Fourier spectral method for nonlinear space-fractional reaction-diffusion equations, *J. Comput. Phys.,* **405** (2020), 109141.

18. H. Zhang, X. Jiang, X. Yang, A time-space spectral method for the time-space fractional Fokker-Planck equation and its inverse problem, *Appl. Math. Comput.,* **320** (2018), 302–318.

19. S. Kazem, S. Abbasbandy, S. Kumar, Fractional-order Legendre functions for solving fractional-order differential equations, *Appl. Math. Model.,* **37** (2013), 5498–5510.

20. A. H. Bhrawya, A. S. Alofi, The operational matrix of fractional integration for shifted Chebyshev polynomials, *Appl. Math. Lett.,* **26** (2013), 25–31.

21. W. Han, Y. M. Chen, D. Y. Liu, X. L. Li, D. Boutat, Numerical solution for a class of multi-order fractional differential equations with error correction and convergence analysis, *Adv. Difference Equ.,* **2018** (2018). Available from: https://doi.org/10.1186/s13662-018-1702-z.

22. S. Kazem, An integral operational matrix based on Jacobi polynomials for solving fractional-order differential equations, *Appl. Math. Model.,* **37** (2013), 1126–1136.

23. S. Z. Rida, A. M. Yousef, On the fractional order Rodrigues formula for the Legendre polynomials, *Adv. Appl. Math. Sci.,* **10** (2011), 509–518.

24. R. A. Khan, H. Khalil, New method based on legendre polynomials for solution of system of fractional order partial differential equations, *Int. J. Comput. Math.,* **91** (2014), 2554–2567.

25. I. Talib, C. Tunc, Z. A. Noor, operational matrices of orthogonal Legendre polynomials and their operational, *J. Taibah Univ. Sci.*, **13** (2019), 377–389.

26. I. Talib, F. B. Belgacem, N. A. Asif, H. Khalil, On mixed derivatives type high dimensional multi-term fractional partial differential equations approximate solutions, *AIP Conference Proceedings*, **1798** (2017). Available from: https://doi.org/10.1063/1.4972616.

27. R. Garrappa, E. Kaslik, M. Popolizio, Evaluation of fractional integrals and derivatives of elementary functions: Overview and tutorial, *Mathematics*, **407** (2019), 1–21.

28. K. Diethelm, N. J. Ford, Numerical solution of the Bagley-Torvik equation, *BIT.,* **42** (2002), 490–507.

29. I. Hashim, O. Abdulaziz, S. Momani, Homotopy analysis method for fractional IVPs, *Commun. Nonlinear Sci. Numer. Simul.,* **14** (2009), 674–684.

30. Z. Odibat, S. Momani, An algorithm for the numerical solution of differential equations of fractional order, *J. Appl. Math. Inform.,* **26** (2008), 15–27.

31. Z. Odibat, S. Momani, Analytical comparison between the homotopy perturbation method and variational iteration method for differentialequations of fractional order, *Int. J. Mod. Phys.,* **22** (2008), 4041–4058.

32. A. Bolandtalat, E. Babolian, H. Jafari, Numerical solutions of multi-order fractional differential equations by Boubaker polynomials, *Open Phys.,* **14** (2016), 226–230.
33. D. Zeidan, S. Govekar, M. Pandey, Discontinuity wave interactions in generalized magnetogasdynamics, *Acta Astronautica*, **180** (2021), 110–114.
34. F. Sultana, D. Singh, R. K. Pandey, D. Zeidan, Numerical schemes for a class of tempered fractional integro-differential equations, *Appl. Numer. Math.,* **157** (2020), 110–134.
35. D. Zeidan, B. Bira, Weak shock waves and its interaction with characteristic shocks in polyatomic gas, *Math. Meth. Appl. Sci.,* **42** (2019), 4679–4687.
36. D. Zeidan, C. K. Chau, T. Tzer-Lu, On the characteristic Adomian decomposition method for the Riemann problem, *Math. Meth. Appl. Sci.,* (2019). Available from: `https://doi.org/10.1002/mma.5798.`
37. E. Goncalves, D. Zeidan, Simulation of compressible two-phase flows using a void ratio transport equation, *Commun. Comput. Phys.,* **24** (2018), 167–203.
38. H. Mandal, B. Bira, D. Zeidan, Power series solution of time-fractional Majda-Biello system using lie group analysis, *Proceedings of International Conference on Fractional Differentiation and its Applications (ICFDA)*, **2018**. Available from: `https://doi.org/10.2139/ssrn.3284751.`
39. E. Goncalves, D. Zeidan, Numerical study of turbulent cavitating flows in thermal regime, *Int. J. Numer. Meth. Fl.*, **27** (2017), 1487–1503.
40. S. Kuila, T. Raja Sekhar, D. Zeidan, On the Riemann problem simulation for the Drift-Flux equations of two-Phase flows, *Int. J. Comput. Methods,* **13** (2016), 1650009.
41. X. Zheng, H. Wang, An error estimate of a numerical approximation to a Hidden-Memory variable-order space-time fractional Diffusion equation, *SIAM J. Numer. Anal.,* **58** (2020), 2492–2514.
42. H. Wang, X. Zheng, Wellposedness and regularity of the variable-order time-fractional diffusion equations, *J. Math. Anal. Appl.,* **475** (2019), 1778–1802.
43. X. Zheng, H. Wang, Optimal-order error estimates of finite element approximations to variable-order time-fractional diffusion equations without regularity assumptions of the true solutions, *IMA J. Numer. Anal.,* **41** (2021), 1522–1545.
44. X. Zheng, H. Wang, An optimal-order numerical approximation to variable-order space-fractional diffusion equations on uniform or graded meshes, *SIAM J. Numer. Anal.,* **58** (2020), 330–352.
45. K. Kumar, R. K. Pandey, S. Sharma, Comparative study of three numerical schemes for fractional integro-differential equations, *J. Comput. Appl. Math.,* **315** (2017), 287–302.

AIMS Press